Islamic Azad University

Journal of

Optoelectronical Nanostructures

Summer 2022 / Vol. 7, No. 3

Research Paper

Data-Driven State Estimation of Carbon Nanotube Field Effect Transistor with Smart RBF Network

Hossein Afkhami[1], Faridoon Shabani Nia*[,2], Jamshid Aghaei[3]

[1] Department of Mechanical, Electrical and Computer Engineering, Science and Research Branch, Islamic Azad University, Tehran, Iran.
[2] Department of Power and Control Engineering, Shiraz University, Shiraz, Iran
3 Department of Electrical and Electronics Engineering, Shiraz University of Technology, Shiraz, Iran

Received: 21 May. 2022
Revised: 25 Jun. 2022
Accepted: 5 Jul. 2022
Published: 15 Sep. 2022

Use your device to scan and read the article online

Keywords:
CNTFET, Modeling, Nonlinear System, RBF, State Estimation

Abstract:
Since 1993, Devices based on CNTs have applications ranging from nanoelectronics to optoelectronics. The challenging issue in designing these devices is that the nonequilibrium Green's function (NEGF) method has to be employed to solve the Schrödinger and Poisson equations, which is complex and time consuming. In the present study, a novel smart and optimal algorithm is presented for fast and accurate modeling of CNT field-effect transistors (CNTFETs) based on an artificial neural network. A new and efficient way is presented for incrementally constructing radial basis function (RBF) networks with optimized neuron radii to obtain the estimator network. An incremental extreme learning machine (I-ELM) algorithm is used to train the RBF network. To ensure the optimal radii for incremental neurons, this algorithm utilizes a modified version of an optimization algorithm known as the Nelder-Mead simplex algorithm. Results confirm that the proposed approach reduces the network size for faster error convergence while preserving the estimation accuracy.

Citation: Hossein Afkhami, Faridoon Shabani Nia, Jamshid. Data-Driven State Estimation of Carbon Nanotube Field Effect Transistor with Smart RBF Network . **Journal of Optoelectronical Nanostructures. 2022; 7 (3): 92- 107**
DOI: 10.30495/JOPN.2022.30232.1262

***Corresponding author:** Faridoon Shabani Nia
Address: Department of Power and Control Engineering, Shiraz University, Shiraz, Iran. **Tell:** 00989173025492 **Email:** shabani@shirazu.ac.ir

1. INTRODUCTION

The performance of electrical circuits can be improved using carbon nanotube (CNT)-based devices [1-3]. This improvement can also be achieved by the diminishment of metal-oxide-semiconductor field-effect transistors (MOSFETs). Conversely, smaller gate lengths can lead to the degradation in the transfer characteristics of planar MOSFETs due to short channel effect[4-7]. To overcome this problem, a favorable alternative to MOSFETs is CNTFETs[8]. In fact, a carbon nanotube is a sheet of graphene rolled into a tube. A CNT may be semiconducting or metallic depending on how the graphene sheet is rolled up [9]. Therefore, CNTs can be an excellent candidate for high-performance transistors. Semiconducting nanotubes, such as single-walled CNTs, have attracted the attention of researchers [10, 11]. The first type of CNTFETs was made of oxidized silicon substrates containing a thick Sio2 layer and a back-gate. This configuration could not provide an appropriate gate control on drain current [11]. The first top gate CNTFET [12] was designed by Wind et al. to achieve a better performance compared to MOSFETs. In [13], the main concepts of quantum transport, such as self-energy and density matrix are explained and the formalism of NEGF is introduced [14, 15]. The results of CNTFET simulations are presented in [16] by developing systematical models of increasing versatility and rigor. Multiscale electronic simulation of CNTs is presented in [17]. This reference focusses on an element of the hierarchy. Moreover, ballistic CNTFETs are simulated in this reference using the solution of Poisson and Schrödinger equations self-consistently based on the NEGF formalism. The main advantages and disadvantages of different CNTFET designs are discussed in [18] using simulation and experimental results. Moreover, the authors of this reference use the findings of the study to evaluate a new well-suited technique, called the tunneling-CNTFET (T-CNTFET) for CNT-based transistor applications. The parameters of power delay product (PDP) and intrinsic switching speed are considered in this research. in [19] an innovative tunnel field-effect transistor (TFET) is discussed. The superior gate controllability makes TFET a promising candidate. In [5], the authors show that the voltage swing and noise margin depend on the supply voltage and tube diameter. Moreover, they found that CNT diameters from 1 to 1.5 nm result in the best ratio of ION-to-IOFF with a noise margin that is good. Reference [20] presents compact single-walled CNTFETs (SW-CNTFETs) with either semiconducting or metallic CNT conducting channel. The results of this reference show that the quantum confinement in axial and circumferential

directions has a screening effect due to parallel CNTs. Reference [21] investigates the self-heating effect in a CNT-based FET and compares the conventional MOSFET structure using Silvaco TCAD software. In [22], it is shown that nonuniformly-doped CNTFETs can suppress ambipolar conduction and band to band tunneling. The energy band calculations confirm improvements in off current and ambipolar behavior. In [23], instead of using NEGF formalism, CNT-MOSFETs are modeled and simulated by utilizing multi-layer perceptron (MLP) networks as an artificial neural network (ANN). The ANN is trained and optimized with the data extracted from the MATLAB script moscnt.1.0. Weights are determined using the back-propagation technique. A fast and accurate sub circuit is proposed based on ANN in CNTFET technology using HSPICE to simulate an inverter circuit and a current source [24]. A multiscale approach is used to model nanodevices for describing the full complexity of these devices, and different transport formalisms are used. Then, the numerical and corresponding experimental results are carefully compared [25]. In [8], the electrical features of nanotube networks are simulated using the Monte Carlo method. Moreover, an equivalent netlist of the networks that does not have the problems of metallic nanotubes is examined through simulation to identify appropriate densities. The conducting channel of FETs is created by depositing CNTs on top of the oxide layer, while the contact is implemented on the back of the substrate. This design can be used in CNTFETs for application to DNA sensing systems in aqueous solutions[26] . In [10], the continuity and charge equations are solved self-consistently, and long-channel CNTFETs are characterized numerically. By applying filed-dependent mobility, the accuracy of simulation is increased. Additionally, in Ref. [10], the dependence of current values on tube diameters in CNTFETs is thoroughly evaluated.

Based on the algorithms introduced in the literature for CNTFET modeling, neural network has many advantages because of fast convergence. Up to now, these algorithms are constructed randomly, so their structures are not optimum and as fast as possible. To address this problem, the present study investigates a new ANN-based approach for CNTFET modeling. Despite their simplicity, single-layer feedforward networks are recognized as universal approximators of nonlinear systems. Their popularity is due to the direct complex nonlinear mapping from the input space to the output. A linear combination of RBFs, including inputs and neuron parameters, yields the network output. Incremental construction of the RBF algorithm reduces the network size significantly. To ensure the optimal radii for incremental neurons, a modified version of the

simplex method known as the simple optimization algorithm is used.

The innovations of the present research are as follows. 1) For properly determining the center of a newly added neuron, the proposed algorithm replaces the conventional random procedure by a purposeful one. This reduces the network size significantly and leads to faster error convergence while preserving accuracy. 2) The proposed algorithm also optimizes the radius of the added neurons using the modified Nelder-Mead simplex algorithm. In this way, the inefficiency of the original algorithm and problem-solving complexities are reduced.

The organization of the rest of this article is as follows. The CNT-MOSFET modeling and the Green's function for carrier transport calculations are presented in Section 2. Then, state estimation in smart grids is presented in Section 2 by focusing on definitions, assumptions, formulation, and optimization algorithms. Section 3 discusses simulation results involving the case study, criteria, and simulation results. Section 4 presents the concluding remarks.

2. CNTFET AND GREEN'S FUNCTION FORMALISM

Figure 1 shows the structure of the device used in the present study. The modeling parameters of the device are the diameter of the nanotube d, the gate dielectric thickness t_{ox}, gate insulator dielectric constant k, source Fermi level E_f, drain control parameter α_d, and gate control parameter α_g. Environmental variables include the temperature T and the starting/ending values of the voltage sweeps, which have recently been added to allow the model to more accurately simulate non-optimal CNTFET devices.

The electron charge, Q_n, is almost independent of V_{ds} and can be obtained based on MOS electrostatics as follows:

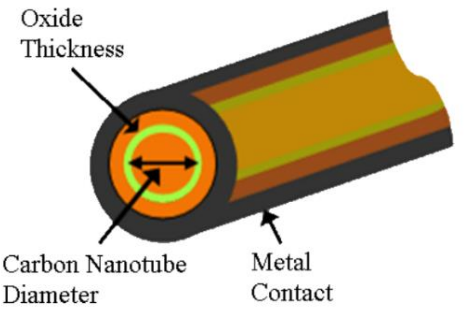

Fig. 1. Structure of CNT-MOSFET

$$Q_n = C_{ox}(V_{gs} - V_t) \quad (1)$$

The electron density at equilibrium at the barrier top can be written as

$$N_o = \int_{-\infty}^{+\infty} D(E) f(E - E_f) dE \quad (2)$$

where f(E-Ef) and D(E) denote the equilibrium Fermi function and the local state density at the barrier top.

The drain current can be calculated from

$$I_D = \int_{-\infty}^{+\infty} J(E)[f_1(\mathrm{E}) - f_2(\mathrm{E})] dE \quad (3)$$

where J(E) denotes the current density of state. This device can be simulated based on the NEGF formalism using the self-consistent solutions of the Schrödinger and Poisson equations [27]. Indeed, non-equilibrium nanoscale systems can be ideally simulated using NEGF formalism [28, 29]. The NEGF-based solution of the Schrödinger equation can be used to determine the charge on CNT surface and the density of states [30]. Then, the solution of Poisson equation and the calculated charge give the new electrostatic potential.

3. INCREMENTAL CONSTRUCTION OF RBF NETWORK

Artificial neural networks, such as single-layer feedforward networks, are used as comprehensive estimators. Despite their simplicity, single-layer feedforward networks provide a direct complex nonlinear mapping from the inputs to linear outputs. Figure 2 depicts the three-layer structure of an RBF network with a single output. The input layer includes N input samples, each with dimension D. Moreover, H activation functions, each in direct relationship with the input samples, are included in the hidden layer. In this study, activation functions are considered to be Gaussian functions of the form[31]:

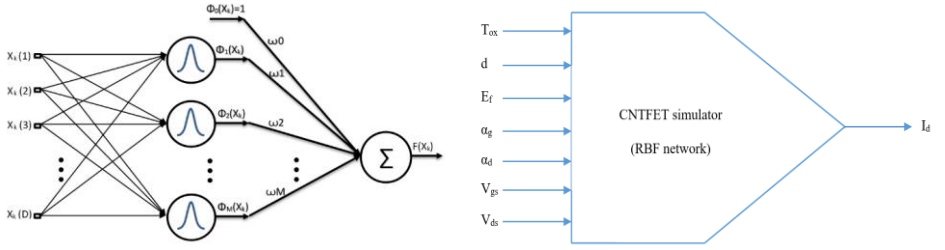

Fig. 2. RBF network for state estimation

$$\varphi_m(x_k) = e^{-\frac{\|c_m - x_k\|}{2\sigma_m^2}} \quad (4)$$

where σm and cm are, respectively, the center and radius of the mth activation function. Network output is a linear combination of activation function outputs in the hidden layer multiplied by their weights. In fact, output weights are the unknowns of the minimization function. The output function can be given as follows:

$$F(x_k) = \sum_{m=1}^{M} \omega_m \varphi_m(x_k) \quad (5)$$

where ω_m is the hidden node's output weight. The model employs the SSE method to minimize the errors while training the network parameters. The objective function is defined as follows:

$$SSE = \frac{1}{2}\sum_{j=1}^{N}(F_d - F(x_k))^2 \quad (6)$$

The aim is to train the neural networks with X(D,N) as inputs and Y(1,N) as outputs of the network. In the trained sample set, at instant k, the network can produce a new output y_k with the dimension of (1,1) for the set of input X_k with the dimension of (D,1). For multiple outputs, it is possible to convert the main problem into problems with single output while training a separate RBF network for every output.

A. Optimization

For the training purposes, three parameters are needed to be adjusted, namely ω_m, σ_m, and c_m. There are various algorithms to determine these parameters and to train the RBF network. One option is to choose neuron centers and their radii randomly and then calculate the output weights through the pseudo-inverse method, which results in a massive training network. Another option is to categorize samples and choose their centers as the node centers, which may result in local optimization. Another approach is to use the supervised learning method to choose the three parameters either by a derivative or directly. The present study uses an incremental pseudo-gradient algorithm because this method is not only a universal approximator but it can also work with a wide range of continuous and discontinuous data as well as derivative and non-derivative functions. It is proven in [32] that for every bounded piecewise non-constant continuous function $\phi: R \to R$ in RBF incremental nodes, for any randomly generated series of functions $\{\phi_m\}$, and for any continuous target function x_i, $lim_{m\to\infty}||x_i - x_m|| = 0$ holds with probability one if

$$\omega_m = \frac{\langle e_{m-1} \cdot \varphi_m \rangle}{\|\varphi_m\|^2} \quad (7)$$

where e_{m-1} is the output error before adding the mth node, and $\langle\ \rangle$ represents the dot product of two vectors.

In this paper, besides calculating the weight of the incremental output node in accordance with the incremental algorithm, the center of each recently added neuron is selected as explained in a scenario in Ref. [31] (see the previous step). This ensures the proper selection of the center and the minimum number of hidden layer neurons. Then, the activation function radius is added and optimized.

Simplex optimization is one of the most popular optimization algorithms for two reasons: first, it provides a direct calculation without derivation. Second, it is simple and efficient for small-scale problems[33].

Basically, this algorithm defines a geometrical structure with (n+1) vertices, where n denotes the number of the optimization problem variables. In every step, the worst vertex is replaced by a new vertex. The worst vertex in terms of optimization function value is reflected through the center of other vertices.

A new geometric shape is formed corresponding to the new function value. This process is repeated until an optimized geometric shape contraction and reflection. Although the method is much simpler to calculate than the derivative-based ones, some errors may occur when calculating large underived data sets. This may lead to a local minimum, and therefore, a reduction in the reliability of the method [34].

To overcome this problem, a modified version of the simplex algorithm is used in this research. Therefore, an extra vertex is used in the basic algorithm

$$x_r . f_r : \begin{cases} f_r < f_0 \rightarrow \text{expansion} \rightarrow x_e . f_e : \begin{cases} f_e < f_0 \rightarrow x_{n+1} = x_e \rightarrow \text{go back to start point} \\ f_e > f_0 \rightarrow x_{n+1} = x_r \rightarrow \text{go back to start point} \end{cases} \\ f_r > f_0 \rightarrow \begin{cases} f_r > f_n \rightarrow \text{contraction} \rightarrow x_c . f_c : \begin{cases} f_c < f_n \rightarrow x_{n+1} = x_c \rightarrow \text{start point} \\ f_c > f_n \rightarrow \text{compression} \rightarrow \text{start point} \end{cases} \\ f_r \leq f_n \rightarrow x_{n+1} = x_r \rightarrow \text{go back to start point} \end{cases} \end{cases}$$

Fig. 3. Diagram of the modified simplex algorithm

to resolve the local minimum issue and to move towards global optimization. The required steps are summarized as follows:

- Formation of a geometric shape with (n + 1) random vertices for a function with n variables
- Formation of an extra vertex with coordinates taken from the diagonal elements of the *n*th leading vertex
- Approximating the gradient at the extra vertex in accordance with other vertices and calculating the reflection point relative to the best point
- Continuing using the basic algorithm.

Figure 3 shows the diagram of this algorithm; the full details of the algorithm are presented in Ref. [35]. After choosing the neuron center and calculating the optimal radius, the output weight of the activation function is computed based on equation (7). The last phase in the training procedure is to check the SSE index, for either stopping or repeating the procedure until reaching an appropriate accuracy.

4. SIMULATION RESULTS

A. Case Study

In the present study, an RBF network is constructed (see Fig. 2) to relate the input vector X_k to the output value yk. The input vector includes d, t_{ox}, k, E_f, α_d, α_g, as well as V_{gs} voltage of gate-source and drain-source voltage V_{ds}. The output is dedicated to the drain current of CNT-MOSFET I_d. The parameter ranges and standard values are summarized in Table 1.

TABLE 1

CNTFET STRUCTURAL PARAMETERS VALUES USED IN SIMULATION

Parameter	Min.	Max.	Standard value
Oxide thickness, t_{ox}, nm	1	30	8
Nanotube diameter, d, nm	0.4	15	1.6
Dielectric constant, k	1	40	20
Series resistance, R_s, ohm	0	10000	0
drain control parameter, αd	0.001	0.1	0.35
Source Fermi level, E_f	-0.01	-0.5	-0.32
Gate control parameter, αg	0.5	1	0.88
Temperature, T, Kelvin	100	450	300

Data samples for training the network are created using the CNTFET environment. To train the RBF network, about 24000 data samples are obtained by the simulation of CNT-MOSFET using CNTFETToy software developed at Purdue University. When a parameter is varied, other parameters are kept at their standard values. Output curves in terms of the input parameters are plotted in Figs. 4 and 5. About 70 percent of data created by CNTFETToy is intended to train RBF network and the remainder is used for testing and validation. Root mean square error of the training process versus time is plotted in Fig. 6.

improvement in the accuracy of the proposed algorithm in comparison with the NEGF one. Mean absolute error is formulated as follows:

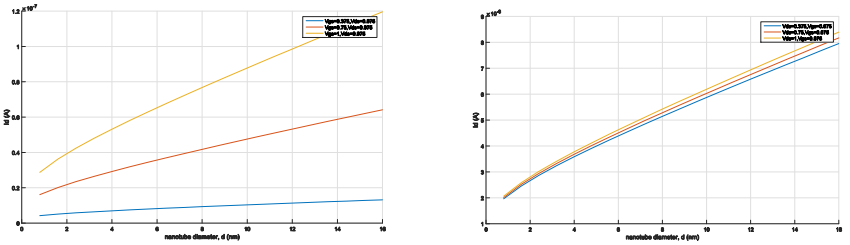

Fig. 4. Current versus the nanotube diameter changes ranging from 0.4 to 16 nm

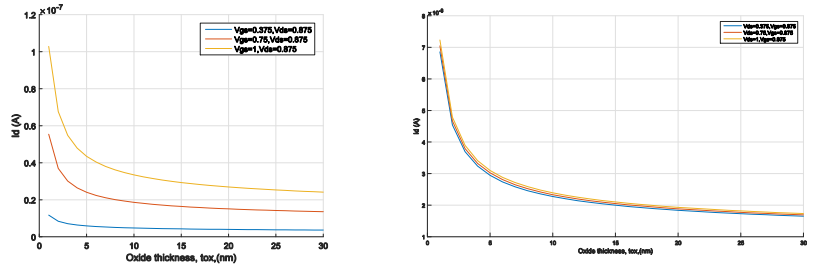

Fig. 5. Current versus the oxide thickness changes ranging from 1 to 30 nm

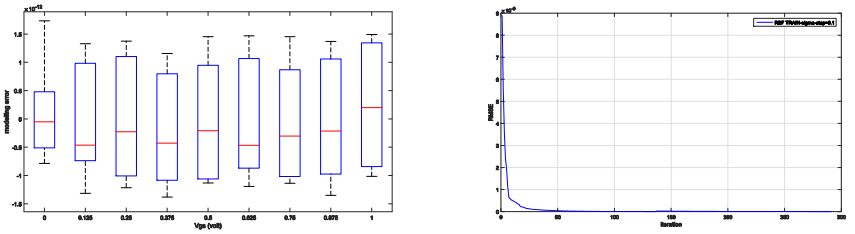

Fig. 6. Boxplot of modeling error using RBF network

$$MAE = \frac{\sum_{i=1}^{n}|x_i - \hat{x}_i|}{n} \quad (8)$$

Root mean squared error is formulated as follows:

$$RMSE = \sqrt{\frac{\sum_{i=1}^{n}(x_i - \hat{x}_i)^2}{n}} \quad (9)$$

The simulation results of drain current versus drain and gate voltages based on the proposed algorithm are plotted in Figs. 7 and 8, respectively. Moreover, a comparison is made between these results and those of the NEGF method. In Fig. 7a, for a fast and accurate modeling of CNTFET characteristics, an incremental step of 0.1 is chosen in the RBF network structure for the sigmoid function. For faster but less accurate modeling, the selected step is equal to 0.2 in Fig. 7b. Although a reduction in training step leads to a larger simulator network, the accuracy is improved considerably while the response time increment is negligible. Figure 8 shows that the RBF network has simulated the I-V curve of CNTFET with high precision.

B. Computational Time

As an effective criterion, the computational time in training and testing phases of the proposed algorithm is compared with that of the NEGF method (Table 2).

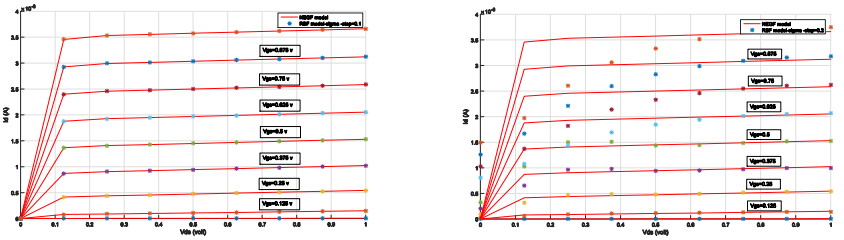

Fig. 7. Id-Vds characteristics with training steps of 0.1 and 0.2.

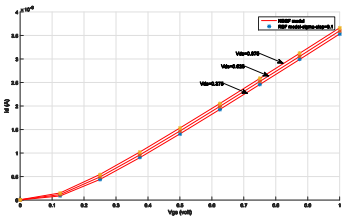

Fig. 8. Id-Vgs characteristics of CNTFET

TABLE 2.

COMPUTATIONAL TIME AND RMSE

Model	CPU time-train (s)	Neurons	CPU time-test (s)	RMSE	
NEGF	--	--	1.2	---	
RBF1	0.19	4-21	0.01	$16*10^{-10}$	
RBF2	4	8-137	0.029	$1*10^{-12}$	

For 0.1 steps of sigmoid function, the proposed algorithm reduces the CPU time by 41 times (0.29 s), while the RMSE is only $1*10^{-12}$. For the second structure of the RBF network with 0.2 steps, the CPU time is 0.01 s, which means 120 times faster performance compared to the NEGF method with an RMSE of $16*10^{-10}$. Therefore, both structures are suitable for fast applications.

5. CONCLUSION

In this study, a new structure of RBF network was proposed for CNTFET modeling. Incremental construction with simple but non-derivative optimization algorithm leads to fast and accurate simulations that justify the use of the RBF network as a universal approximator and the framework of the proposed algorithm. For fast and accurate online simulation of CNTFETs in practical applications, a purposeful and optimal incremental construction was used for the RBF network to guarantee the minimum size of the estimator network. Moreover, the output weights were adjusted using the pseudo-inverse method, and the centers and radii of all newly added neurons were optimized via the modified version of the simplex algorithm to improve the performance. According to the simulation results, the proposed algorithm gives accurate results and reduces the computational time considerably compared to the conventional NEGF method.

ACKNOWLEDGMENT

The authors would like to thank the Purdue University for the development of CNTFETToy software for CNTFET simulation and analysis, which validate the results of this research.

REFERENCES

[1] H. hashemi madani. M. R. Shayesteh. and M. R. Moslemi. A Carbon Nanotube (CNT)-based SiGe Thin Film Solar Cell Structure. Journal of Optoelectronical Nanostructures. 6(1) (2021) 71-86.

Available: https://dx.doi.org/10.30495/jopn.2021.4541

[2] O. Talati Khoei and R. Hosseini. Device and Circuit Performance Simulation of a New Nano-Scaled Side Contacted Field Effect Diode Structure. Journal of Optoelectronical Nanostructures. 4(3) (2019) 17-32.

Available: https://dorl.net/dor/20.1001.1.24237361.2019.4.3.2.4

[3] H. Faezinia and M. zavvari. Quantum modeling of light absorption in graphene based photo-transistors. Journal of Optoelectronical Nanostructures. 2(1) (2017) 9-20.

Available: https://dorl.net/dor/20.1001.1.24237361.2017.2.1.2.6

[4] A. rezaei. B. Azizollah-Ganji. and M. Gholipour. Effects of the Channel Length on the Nanoscale Field Effect Diode Performance. Journal of Optoelectronical Nanostructures. 3(2) (2018) 29-40.

Available: https://dorl.net/dor/20.1001.1.24237361.2018.3.2.3.6

[5] A. Raychowdhury. A. Keshavarzi. J. Kurtin. V. De. and K. Roy. Carbon Nanotube Field-Effect Transistors for High-Performance Digital Circuits. IEEE Transactions on Electron Devices. 53(11) (2006) 2711-2717.

Available: https://doi.org/10.1109/TED.2006.883816

[6] S. Jogad. H. I. Alkhammash. N. Afzal. and S. A. Loan. CNTFET-based active grounded inductor using positive and negative current conveyors and applications. International Journal of Numerical Modelling. 34(5) (2021) 2895.

available: https://doi.org/10.1002/jnm.2895

[7] S. O. Koswatta. D. E. Nikonov. and M. S. Lundstrom. Computational study of carbon nanotube p-i-n tunnel FETs. Presented at IEEE International Electron Devices Meeting. (2005).

Available:https://doi.org/10.1109/IEDM.2005.1609396

[8] M. Diez-Garcia. A. Vincent. N. Izard. and D. Querlioz. Monte Carlo simulations of carbon nanotube networks for optoelectronic applications. Presented at IEEE International Electron Devices Meeting. (2014).

Available:https://doi.org/10.1109/IEDM.2005.1609396

[9] J. Guo. S. O. Koswatta. N. Neophytou. and M. Lundstrom. Carbon Nanotube Field-Effect Transistors. International Journal of High Speed Electronics and Systems. 16(04) (2006) 897-912.

Available: https://doi.org/10.1142/S0129156406004077

[10] S. Dehghani. Numerical Study of Long Channel Carbon Nanotube Based Transistors by Considering Variation in CNT Diameter. Journal of Nano Research. 61 (2020) 78-87.

Available:https://doi.org/10.4028/www.scientific.net/JNanoR.61.78

[11] K. Bikshalu. V. S. K. Reddy. P. C. S. Reddy. and K. V. Rao. High-performance Carbon Nanotube Field Effect Transistors with High k Dielectric Gate Material. Proceedings. 2(9) (2015) 4457-4462.

Available:https://doi.org/10.1016/j.matpr.2015.10.048

[12] R. Martel. T. Schmidt. H. R. Shea. T. Hertel. and P. Avouris. Single- and Multi-Wall Carbon Nanotube Field-Effect Transistors. Applied Physics Letters. 73 (1998) 10-26.

Available:https://doi.org/10.1063/1.122477

[13] S. Datta. Nanoscale device modeling: the Green's function method. Superlattices and Microstructures. 28(4) (2000) 253-278.

Available:https://doi.org/10.1006/spmi.2000.0920

[14] M. Akbari Eshkalak and R. Faez. A Computational Study on the Performance of Graphene Nanoribbon Field Effect Transistor. Journal of Optoelectronical Nanostructures. 2(3) (2017) 1-12.

Available:https://doi.org/10.1109/DRC.2010.5551931

[15] M. Jafari. Electronic Transmission Wave Function of Disordered Graphene by Direct Method and Green's Function Method. Journal of Optoelectronical Nanostructures. 1(2) (2016) 57-68.

Available:https://dorl.net/dor/20.1001.1.24237361.2016.1.2.6.5

[16] D. L. John. Simulation studies of carbon nanotube field-effect transistors. Text, 2006.
Available:http://hdl.handle.net/2429/18554

[17] J. Guo. S. Datta. M. s. Lundstrom. and M. Anantram. Toward Multiscale Modeling of Carbon Nanotube Transistors. International Journal for Multiscale Computational Engineering 2 (2004) 257-276.

Available:http://dx.doi.org/10.1615/IntJMultCompEng.v2.i2.60

[18]J. Appenzeller. L. Yu-Ming. J. Knoch. C. Zhihong. and P. Avouris. Comparing carbon nanotube transistors - the ideal choice: a novel tunneling device design. IEEE Transactions on Electron Devices. 52(12) (2005) 2568-2576.

Available:https://doi.org/10.1109/TED.2005.859654

[19] Z. Ahangari. Switching Performance of Nanotube Core-Shell Heterojunction Electrically Doped Junctionless Tunnel Field Effect Transistor. Journal of Optoelectronical Nanostructures. 5(2) (2020) 1-12.

Available:https://dorl.net/dor/20.1001.1.24237361.2020.5.2.1.8

[20] J. Deng and H. P. Wong. A Compact SPICE Model for Carbon-Nanotube Field-Effect Transistors Including Nonidealities and Its Application—Part I: Model of the Intrinsic Channel Region. IEEE Transactions on Electron Devices. 54 (12) (2007) 3186-3194.

Available:https://doi.org/10.1109/TED.2007.909043

[21] K. Pourchitsaz and M. R. Shayesteh. Self-heating effect modeling of a carbon nanotube-based fieldeffect transistor (CNTFET). Journal of Optoelectronical Nanostructures. 4(1) (2019) 51-66.

Available:https://dorl.net/dor/20.1001.1.24237361.2019.4.1.4.2

[22] I. Hassaninia. M. H. Sheikhi. and Z. Kordrostami. Simulation of carbon nanotube FETs with linear doping profile near the source and drain contacts. Solid-State Electronics. 52(6) (2008) 980-985.

Available:https://doi.org/10.1016/j.sse.2008.01.021

[23] M. Hayati. A. Rezaei. and M. Seifi. CNT-MOSFET modeling based on artificial neural network: Application to simulation of nanoscale circuits. Solid-State Electronics. 54 (2010) 52-57.

Available:https://doi.org/10.1016/j.sse.2009.09.027

[24] R. Abdollahzadeh Badelbo. F. Farokhi. and A. Kashaniniya. Efficient Parameters Selection for CNTFET Modelling Using Artificial Neural

Networks. International Journal of Smart Electrical Engineering. 2(4). (2013) 217-222.

Available:https://dorl.net/dor/20.1001.1.22519246.2013.02.4.5.4

[25] C. Maneux et al.. Multiscale simulation of carbon nanotube transistors. Solid-State Electronics. 89 (2013) 26-67.

Available:https://doi.org/10.1016/j.sse.2013.06.013

[26] T. Chu. N. Thuy. T. Tran. T. Huyen. and A. T. Mai. Carbon Nanotube Field-Effect Transistor for DNA Sensing. Journal of Electronic Materials. 46 (2017) 01-05.

Available:https://link.springer.com/article/10.1007/s11664-016-5238-2

[27] S. Koswatta. M. s. Lundstrom. M. Anantram. and D. Nikonov. Simulation of phonon-assisted band-to-band tunneling in carbon nanotube field-effect transistors. Applied Physics Letters. 87 (2005) 253107-253107.

Available:http://dx.doi.org/10.1063/1.2146065

[28] S. Datta, Atom to Transistor, in Quantum Transport. Cambridge: Cambridge University Press, 2005.

Available:https://doi.org/10.1017/CBO9781139164313

[29] J. Guo and M.s. Lundstrom, Device Simulation of SWNT-FETs. 2009, 107-131.

Available:https://link.springer.com/chapter/10.1007/978-0-387-69285-2_5

[30] Y. Sun et al.. Suspended CNT-Based FET sensor for ultrasensitive and label-free detection of DNA hybridization. Biosensors and Bioelectronics. 137 (2019) 255-262.

Available:https://doi.org/10.1016/j.bios.2019.04.054

[31] P. Reiner and B. M. Wilamowski. Efficient incremental construction of RBF networks using quasi-gradient method. Neurocomputing. 150 (2015) 349-356.

Available:https://doi.org/10.1016/j.neucom.2014.05.082

[32] G.-B. Huang. L. Chen. and C.-K. Siew. Universal approximation using incremental constructive feedforward networks with random hidden nodes. Trans. Neur. Netw.. 17(4) (2006) 879-892.

Available:http://dx.doi.org/10.1109/TNN.2006.875977

[33] Y. Weng. R. Negi. and M. D. Ilić. A search method for obtaining initial guesses for smart grid state estimation. Presented at 2012 IEEE Third International Conference on Smart Grid Communications (SmartGridComm). (2012).

Available:https://doi.org/10.1109/SmartGridComm.2012.6486051

[34] J. Lagarias. J. Reeds. M. Wright. and P. Wright. Convergence Properties of the Nelder-Mead Simplex Method in Low Dimensions. SIAM Journal on Optimization. 9(1) (1998) 112-147.

Available:http://dx.doi.org/10.1137/S1052623496303470

[35] N. D. Pham. Improved Nelder Mead's Simplex Method and Applications. Doctor of Philosophy. Auburn 2012.

Available:http://hdl.handle.net/10415/2985